Inertia-gravity waves in the troposphere and lower stratosphere associated with a jet stream exit region

L. Thomas, R. M. Worthington, A. J. Mcdonald

Ann. Geophysicae 17, 115–121 (1999) © EGS – Springer-Verlag 1999

Annales Geophysicae

Inertia-gravity waves in the troposphere and lower stratosphere associated with a jet stream exit region

L. Thomas, R. M. Worthington and A. J. McDonald

Department of Physics, University of Wales, Aberystwyth, Ceredigion SY23 3BZ, UK

Received: 6 November 1997 / Revised: 10 June 1998 / Accepted: 11 June 1998

Abstract. Radar measurements at Aberystwyth (52.4°N, 4.1°W) of winds at tropospheric and lower stratospheric heights are shown for 12–13 March 1994 in a region of highly curved flow, downstream of the jet maximum. The perturbations of horizontal velocity have comparable amplitudes in the troposphere and lower stratosphere with downward and upward phase propagation, respectively, in these two height regions. The sense of rotation with increasing height in hodographs of horizontal perturbation velocity derived for hourly intervals show downwards propagation of energy in the troposphere and upward propagation in the lower stratosphere with vertical wavelengths of 1.7 to 2.3 km. The results indicate inertia-gravity waves propagating in a direction similar to that of the jet stream but at smaller velocities. Some of the features observed contrast with those of previous observations of inertia-gravity waves propagating transverse to the jet stream. The interpretation of the hodographs to derive wave parameters has taken account of the vertical shear of the background wind transverse to the direction of wave propagation.

Key words. Meteorology and atmospheric dynamics (mesoscale meteorology; middle atmosphere dynamics; waves and tides)

1 Introduction

Radar observations often show the presence of wave-like structures in height variations of wind speeds. These structures typically have rather small vertical wavelengths (≤3.0 km) and periods of several hours. The common interpretation of these structures has been in terms of inertia-gravity waves (Cornish and Larsen, 1989; Thomas *et al.*, 1992; Maekawa *et al.*, 1984; Sato, 1994), such waves having previously been identified in quasi-periodic fluctuations of wind speeds identified by balloons (Thompson, 1978; Cadet and Teitelbaum, 1979). However, Hines (1989) has proposed an alternative interpretation of the radar observations of Sato and Woodman (1982), analysed and interpreted by Maekawa *et al.* (1984), in terms of quasi-stationary waves generated orographically by airflow over the island and mountains of Puerto Rico. The roles of mountain waves and inertia-gravity waves in other observations at Puerto Rico have since been the subjects of considerable discussion (Cornish and Larsen, 1989; Hines, 1995a, b; Larsen, 1995).

Radar observations of long-period waves have shown a preference for meridional propagation in the lower stratosphere (Hirota and Niki, 1986; Yamanaka *et al.*, 1989; Thomas *et al.*, 1992; Prichard and Thomas, 1993). Studies of hodographs (e.g. Cornish and Larsen, 1989) and cross spectra (Cho, 1995) have shown upwards energy propagation in the lower stratosphere and downwards propagation of energy below the tropopause (Thomas *et al.*, 1992). These latter workers identified tentatively a source associated with a jet stream to the north. Two and three-dimensional model studies by Fritts and Luo (1992) and Luo and Fritts (1993), respectively, have supported the suggestion that geostrophic adjustment of the jet stream may provide a significant source of inertia-gravity waves and help explain the preference for meridional propagation. However, a statistical study of the meridional propagation of waves, observed with the MU radar, relative to the jet axis, as identified in ECMWF operational data, by Sato (1994) suggested that the geostrophic adjustment process just at the jet axis is not the dominant generation mechanism.

A notable feature of the balloon (Thompson, 1978; Cadet and Teitelbaum, 1979) and radar results (Thomas *et al.*, 1992; Sato, 1994; Cho, 1995), apart from the commonly observed downward propagation of phase in the lower stratosphere, was the low intensity or absence of the inertia-gravity waves at heights below the jet stream. The present study, which is based on data

provided by the NERC MST radar facility at Aberystwyth (52.4°N, 4.1°W), is concerned with a long-period wave event during 12 and 13 March, 1994. It is argued that this is not related to mountain-wave activity and, instead, represents an inertia-gravity wave, but with rather different characteristics from those observed previously.

2 Radar system and observations

The radar system operates at a frequency of 46.5 MHz, has a peak power of 160 kW and a duty cycle of 2.5%. The antenna array is made up of 400 four-element Yagis occupying an area of 1.1×10^4 m^2, providing a one-way beamwidth of 3°. A total of 16 beam directions are available, but the present investigation makes use of those in the vertical and 6° to the vertical in azimuths near NE and NW. The measurements were carried out with 8 μs pulses, coded with a baud length of 2 μs, the receiver being gated at 1 μs intervals. For each beam direction, the radial velocities were observed for periods of 21s which were repeated in cycle times of 2.4-min, averages over 12-min intervals being used in the present study.

3 Analysis of data

3.1 Mean and perturbation velocities

Figure 1a shows the variation with height and time of the horizontal wind vector during the period 0000 UT on 12 March, 1994 to 0000 UT on 14 March, 1994. The wind veers with increasing height up to about the tropopause, near 12 km, during the first 24 h at which time the wind at the lowest height, near 2.5 km, also shows a clockwise rotation. Figure 1b shows the corresponding contours of vertical velocity. The large amplitude and slowly varying phase are common features of mountain waves at this site and their presence is confirmed by the characteristic frequency spectra observed throughout the height range shown (Worthington and Thomas, 1996). It is to be noted that in both the horizontal wind and vertical velocity plots the height and time resolutions are degraded from the initial measurements for the purpose of clarity.

The height profiles of horizontal wind for 12-min intervals were subjected to a fourth-order Butterworth high-pass filter to remove variations with vertical scales greater than 5 km, and time filtering served to reveal fluctuations in the 2–10 h period band. Figure 2a, b

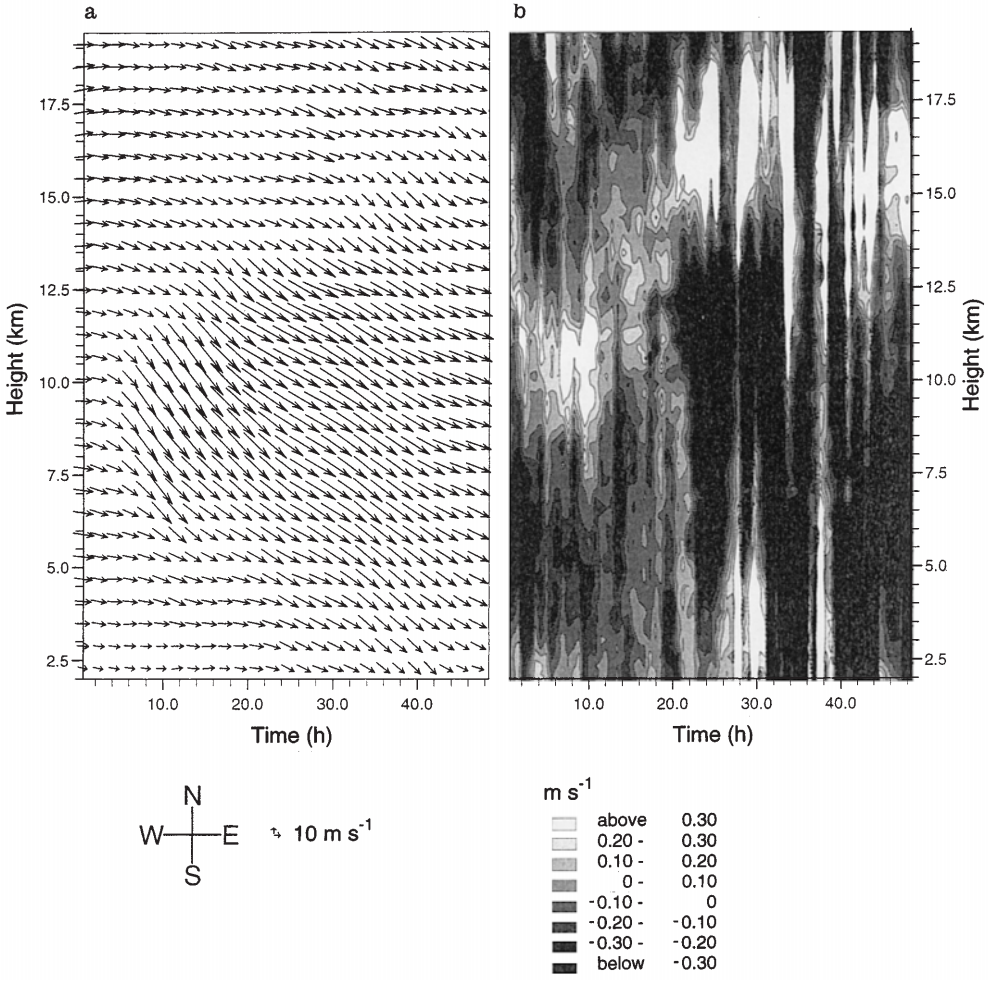

Fig. 1a, b. Height-time plots of **a** background-wind velocity and **b** contours of vertical velocity, for 12–13 March, 1994

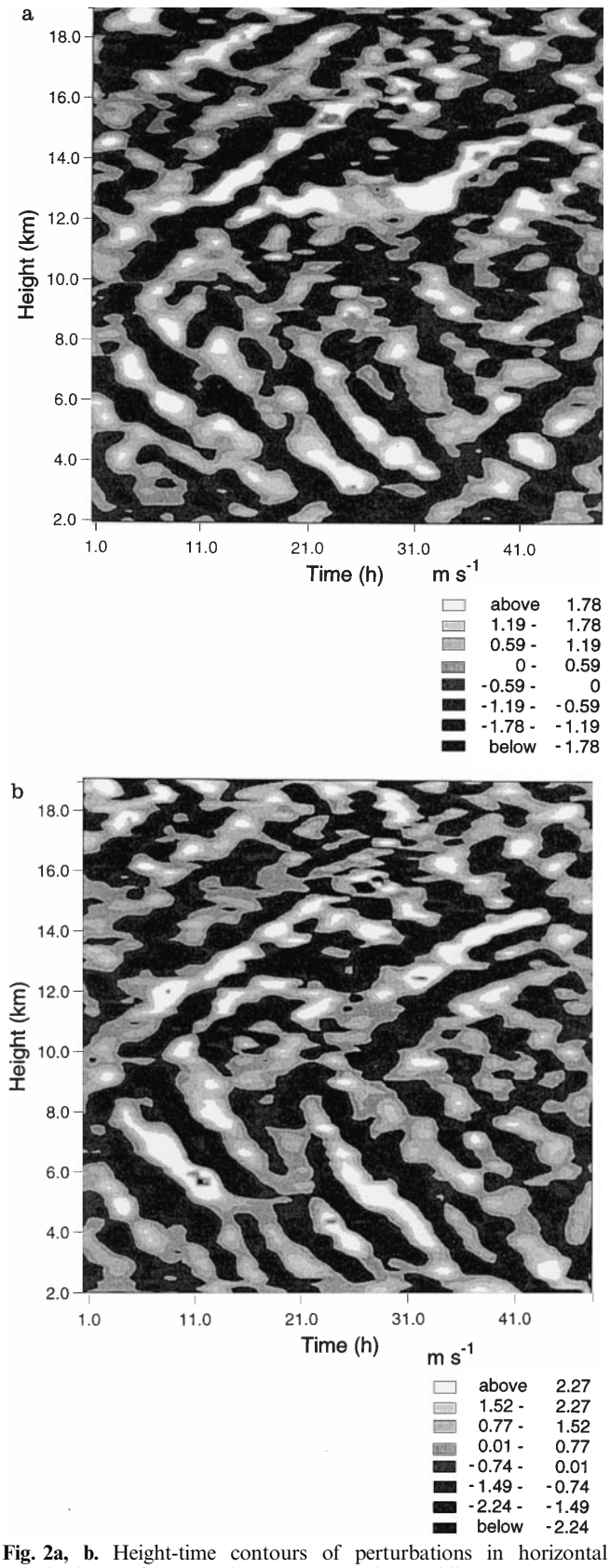

Fig. 2a, b. Height-time contours of perturbations in horizontal velocity in m/s for **a** zonal component and **b** meridional component, for 12–13 March, 1994

shows height-time contours of horizontal velocity perturbations in the zonal and meridional directions, respectively, for the 48 h of observation. Alternating positive and negative perturbations of amplitudes about 2 m/s are observed in both components with a vertical structure of 2–3 km in the troposphere and about 2 km in the lower stratosphere. Clear downward propagation of disturbance is apparent at heights below 9–10 km and upward propagation at heights above this level. The corresponding periods are 9 h and 10 h, respectively.

The location of the radar site on the west coast of Wales in relation to the jet stream is illustrated by reference to the contour map of zonal and meridional velocities for the 315 K isentrope level, at about 11–12 km, for 1200 UT on 12 March 1994, as given by the ECMWF operational analysis, Fig. 3a, b. The tightly curved flow downstream of the jet maximum moves eastward with time almost parallel to latitude circles, and corresponds to the jet stream exit region described by O'Sullivan and Dunkerton (1995) in their theoretical study of associated inertia-gravity waves.

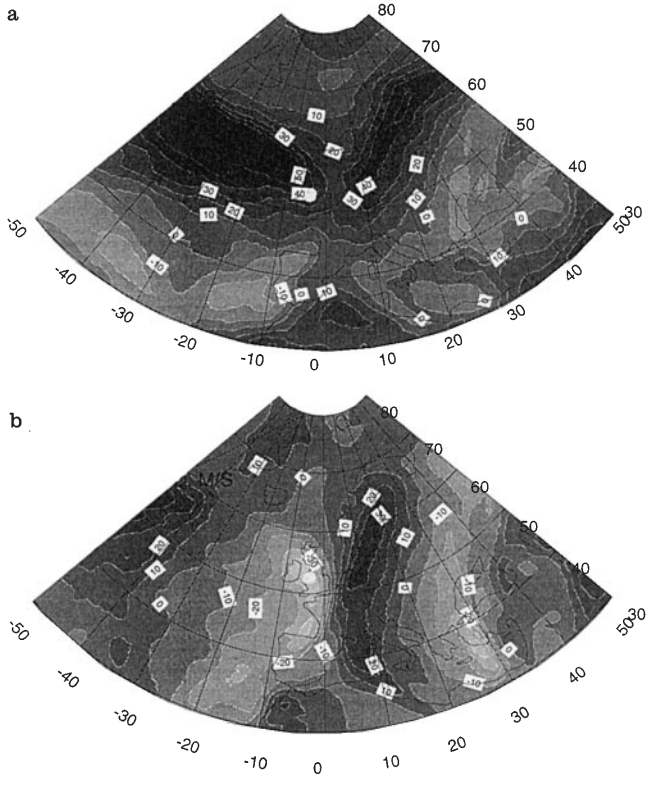

Fig. 3a, b. Contour plots of horizontal wind velocities in m/s for the 315 K isentrope level, as given by the ECMWF operational analysis at 1200 UT on 12 March, 1994, for **a** zonal component and **b** meridional component, in which the position of Aberystwyth (52.4°N, 4.1°W) is indicated by a *white dot*

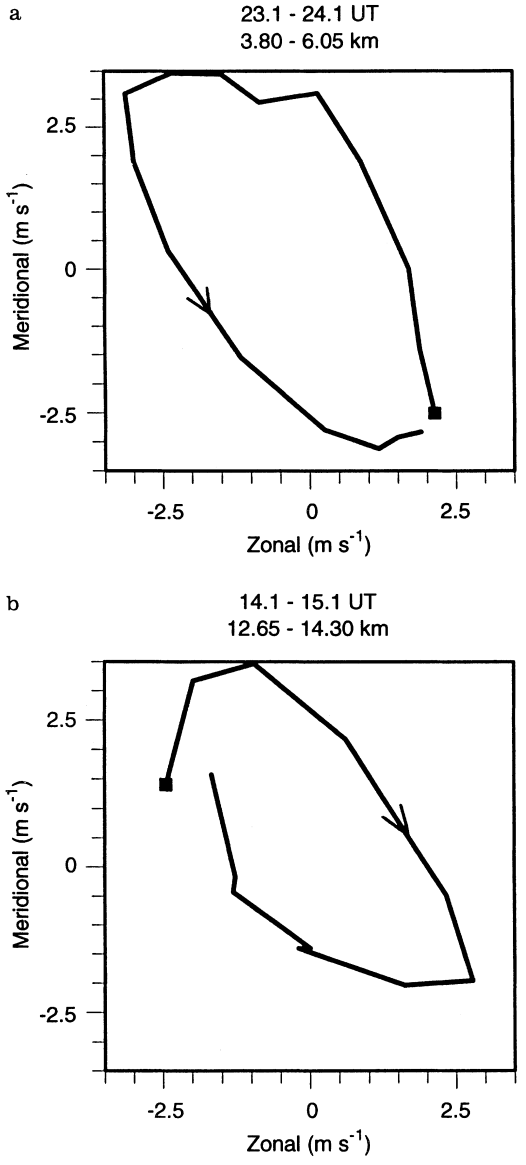

Fig. 4a, b. Hodographs of perturbation velocity for heights **a** below the tropopause, and **b** above the tropopause, based on mean values over 1.0 h and 150 m increasing height intervals, on 12 March 1994. The lowest heights are marked by *solid squares* and the directions of rotation with increasing heights are indicated by *arrows*

3.2 Hodographs of perturbation velocities

Figure 4a, b shows examples of the joint variation of the zonal and meridional perturbation velocities with height at intervals of 150 m. Each variation refers to mean values derived for periods of one hour from individual 12-min samples, the total uncertainty for each value being about 1 m/s in each component; the lowest heights are indicated by solid squares. It can be seen that the first case, beginning at a height of 3.80 km for the interval 23.1–24.1 UT on 12 March, shows an elliptical form and anticlockwise rotation of the perturbation wind vector with increasing height, Fig. 4a. Consideration of the dispersion and polarisation relations (e.g. Thompson, 1978) shows that this sense of rotation in the Northern Hemisphere corresponds to a downward propagation of energy. In contrast, the variation for heights above 12.65 km for the interval 14.1–15.1 UT on 12 March in the second case shows a clockwise rotation with increasing height, Fig. 4b, and corresponds to an upward propagation of energy. From the more detailed information on the reversal of the vertical phase propagation, Sect. 3.1, it seems that the wave source would be at 9–10 km, near the height of maximum horizontal velocity, and could again be associated with the jet stream. The studies of other height and time intervals have shown more poorly defined hodographs but provide additional evidence for anticlockwise and clockwise rotations below and above the interval 10–12 km, respectively. As in the examples shown in Fig. 4a, b, the hodographs are commonly orientated with the major axes in the NW-SE azimuth.

The results of Figs. 2a, b and 4a, b indicate that in the troposphere the vertical components of phase and group velocities are both downward and in the lower stratosphere they are both upward. This implies that for both height ranges the observed and intrinsic wave frequencies are of opposite sign. The relationship between the observed frequency, ω_o, and the intrinsic frequency, ω, of the wave is given by the Doppler expression:

$$\omega_o = \omega + kU \qquad (1)$$

where U is the mean background wind component in the direction of wave propagation and k is the horizontal wave number.

According to linear theory (e.g. Thompson, 1978), the horizontal direction of propagation is parallel to the major axis of the polarisation ellipse. The difference in sign between ω_o and ω indicates that the observed wave propagation is south-eastward at a phase velocity less than the background wind value U and the intrinsic phase propagation is north-westward. Unfortunately, with the vertical velocities being dominated by mountain-wave activity, the use of the maximum perturbation velocities in the vertical and horizontal directions to confirm this wave propagation direction (e.g. Tsuda *et al.*, 1990; Thomas *et al.*, 1992) is not possible.

A contribution to the polarisation ratio, given by the ratio of the minor to major axis of the elliptical hodograph, can arise from the vertical shear of the background wind transverse to the direction of wave propagation (dV/dz), i.e. to the major axis of the ellipse, (Hines, 1989). This contribution is given by $N^{-1}\, dV/dz$, where N represents the angular Brunt-Väisälä frequency. Thus for the tropospheric case, Fig. 4a, for which the polarisation ratio is 0.5 and the Brunt-Väisälä frequency derived from radiosonde temperature measurements is 0.013 rad/s, a gradient of 6.5×10^{-3} m/s/m would be required to account fully for this ratio; the corresponding figure for the lower stratospheric case is 8.4×10^{-3} m/s/m. These values are substantially larger than the observed gradients for these two cases but such large shears dominate the polarisation ratios for certain hodographs, especially in the lower stratosphere.

3.3 Estimation of wave parameters

As mentioned in Sects. 1 and 3.2, Hines (1989) drew attention to the need to take account of the vertical wind shear in the background horizontal wind perpendicular to the horizontal wave vector in the interpretation of observed elliptical polarisations of velocity perturbations.

The ratio of minor to major axis of the ellipse is then given by

$$R = \left| \frac{f}{\omega} - \frac{k}{m\omega} \frac{\mathrm{d}V}{\mathrm{d}z} \right| \tag{2}$$

where f is the Coriolis parameter, 1.156×10^{-4} rad/s at Aberystwyth, and m is the vertical wave number.

We adopt the convention that the intrinsic frequency, ω, is positive, k is orientated parallel to the major axes of the hodographs and directed towards the north west, U and V represent the background wind parallel and perpendicular to k, V being towards the southwest, and m is positive in the troposphere and negative in the lower stratosphere.

The dispersion relation is given by a simplification of a general form presented by Kunze (1985):

$$\omega^2 = f^2 + \frac{N^2 k^2}{m^2} - 2f \frac{k}{m} \frac{\mathrm{d}V}{\mathrm{d}z} \tag{3}$$

The situation of primary interest is that in which the expression within the modulus sign of Eq. (2) is positive, and substituting for k/m in Eq. (3) gives

$$\omega = \frac{fR\left(N^2 - \left(\frac{\mathrm{d}V}{\mathrm{d}z}\right)^2\right) \pm f \frac{\mathrm{d}V}{\mathrm{d}z} \left\{ \left(N^2 - \left(\frac{\mathrm{d}V}{\mathrm{d}z}\right)^2\right)(1 - R^2) \right\}^{1/2}}{N^2 R^2 - \left(\frac{\mathrm{d}V}{\mathrm{d}z}\right)^2} \tag{4}$$

With the values of observed parameters relating to the two cases represented in Fig. 4a, b, corresponding values of ω are derived as indicated in Table 1. The hourly mean profiles of horizontal wind velocity show considerable vertical structure and there are some uncertainties in the gradients, $\mathrm{d}V/\mathrm{d}z$, of the velocity perpendicular to the major axes of the ellipses, especially in the second case, Fig. 4b. Here the gradient 4×10^{-3} m/s/m shown is for the lower part of the height range, between 12.65 km and 13.8 km, a value near zero being shown between 13.8 and 14.3 km. In the calculations for this case the two values are assumed, in turn, to relate to the full height range 12.65 to 14.30 km. The zero gradient results for ω and k for the two cases, Fig. 4a, b, are shown bracketed in Table 1.

In applying Eq. (4) for the non-zero values of $\mathrm{d}V/\mathrm{d}z$ shown, the first terms in the numerators are the largest and the derived values of ω are all positive. The larger magnitude of $\mathrm{d}V/\mathrm{d}z$ in the second case, Fig. 4b, renders the values of the two terms in the numerator more similar and these then yield dissimilar values of ω, Table 1. For certain other hodographs the interpretation is compromised by large values of $|\mathrm{d}V/\mathrm{d}z|$.

A knowledge of m permits the estimation of k:

$$k = \frac{fm}{N^2} \frac{\mathrm{d}V}{\mathrm{d}z} \pm \frac{m}{N} \left[\frac{f^2}{N^2} \left(\frac{\mathrm{d}V}{\mathrm{d}z}\right)^2 + \omega^2 - f^2 \right]^{1/2} \tag{5}$$

Similar expressions to Eqs. (2)–(5) have been shown by Cho (1995). With the substitution of the derived values of ω, for each of the two cases considered, it is found that the term including the square bracket has the larger magnitude. Consequently for each value of ω, both positive and negative values of k are obtained. With the coordinate system adopted, the positive values of k are appropriate and are indicated in Table 1.

The value of the background wind velocity in the direction of wave propagation provides an independent estimate of k from the Doppler relation Eq. (1). With estimates of U relating to the hourly mean values in the directions of the major axes of the ellipses in Fig. 4a, b, the values of $2\pi/k$ derived for the two cases are found to be substantially larger than the corresponding values derived from Eq. (5). Uncertainties in the values of ω_o adopted in Eq. (1) make little contributions to the differences between the two sets of values.

It is to be noted that the velocity magnitude of 33 m/s in the first case relates to the mean for the height interval 3.80–6.05 km during the hour 23.1–24.1 UT on 12 March. The relevance of this value to the interpretation of the corresponding hodograph needs to be examined. The vertical component of the group velocity, $d\omega/dm$, can be derived from Eq. (3). For the values of 7.0 h for $2\pi/\omega$ and 136 km for $2\pi/k$ shown for this case in Table 1, a value of 0.068 m/s is derived for this velocity, with the wind gradient term contributing about 2%. Thus the time taken for the downward propagation of waves from 6.05 km to 3.80 km is 9.2 h. The value of U to be adopted in Eq. (1), and also the value of $\mathrm{d}V/\mathrm{d}z$ incorporated in Eqs. (4) and (5), should then be representative of the period from about 1500 UT to 2400 UT and not just 23.1 UT to 24.1 UT. The reconciliation of the two values of k requires a reduction in the magnitude of U to about 10 m/s. An examination of the wind vectors in the height range 3.80 to 6.05 km, Fig. 1a, does suggest a reduction of the velocity component in the direction of the major axis of the ellipse in Fig. 4a for several hours prior to the interval 23.1–24.1 UT, arising both from a decrease in magnitude and a change in direction of the total wind. The mean U profile for the period 1500 UT to 2400 UT shows a

Table 1. Estimated magnitudes of wave parameters

	a	b
Time, UT	23.1–24.1	14.1–15.1
Height, km	3.80–6.05	12.65–14.30
N, rad/s	0.013	0.021
R	0.5	0.4
U, m/s	33	30
$\frac{\mathrm{d}V}{\mathrm{d}z}$ 10^{-4} m/s/m	5.2	40.0
$2\pi/\omega_o$, h	8.8	10.0
$2\pi/m$, km	2.25	1.65
$2\pi/\omega$, h, (from Eq. 4)	7.0, 8.1, (7.5)	3.4, 8.7, (6.0)
$2\pi/k$, km (from Eq. 5)	136, 164, (146)	71, 243, (131)

range of magnitudes from 10 m/s to 35 m/s over the 3.80 km to 6.05 km height range. The values of ω and k derived from Eqs. (4) and (5), respectively, with the mean value of $\mathrm{d}V/\mathrm{d}z$ for the same period were rather similar to those shown in Table 1, implying that the values of $2\pi/k$ derived from Eq. (1) are larger than the corresponding values derived from Eq. (5), as previously. A similar argument could be applied for the second case, Fig. 4b, but the required reduction in U is less clear.

4 Discussion

The height-time variation of vertical velocity presented in Fig. 1b is typical of mountain waves at Aberystwyth (Prichard *et al.*, 1995; Worthington and Thomas, 1996), although they often do not extend to such great heights. Before considering the overall results in terms of inertia-gravity waves, it needs to be established that the observations do not reproduce the situation highlighted by Hines (1989), namely that orographically generated quasi-stationary mountain waves with suitable gradients in the wind transverse to the wave propagation direction, $\mathrm{d}V/\mathrm{d}z$, can simulate the observations of inertia-gravity waves and, specifically, the rotation with height of the horizontal wind-perturbation.

It is evident that the sign of the gradient, $\mathrm{d}V/\mathrm{d}z$, at heights below and above the jet stream could be such as to contribute rotations of opposite sign in these two regions. However, the contribution of the gradient term to the polarisation relation is given by $\left|\frac{1}{N}\frac{\mathrm{d}V}{\mathrm{d}z}\right|$, which for the tropospheric case, a in Table 1, amounts to 0.04, only 8% of the observed ratio; for the lower stratospheric case b where, as indicated previously, the magnitude of the overall gradient was believed to be less than the value 4×10^{-3} m/s/m, shown in Table 1, the contribution is less than the corresponding value of 0.19, i.e. 48% of the observed ratio.

Hines (1989) has suggested that monotonic changes in the background wind and/or temperature in the region between the ground and the observing level could provide for a quasi-stationary mountain wave a downward progression of phase which is sometimes interpreted in terms of an inertia-gravity wave. In the present study, both downward and upward progressions of phase are observed, Fig. 2a, b. Furthermore, the vertical velocity measurements in Fig. 1b, and in similar events, show vertical wavelengths of about 14 km with no evidence of a steady phase propagation throughout the observation period, and clear vertical phase propagation in the horizontal velocity perturbations has sometimes been observed at heights above critical layers for mountain waves.

The direction of wave propagation relative to that of the jet stream is of interest in considerations of possible source mechanisms. It is, therefore, useful to examine whether the hodographs of Fig. 4a, b could be interpreted in terms of waves propagating transverse rather than parallel to the jet stream. The corresponding alignments of the horizontal wave vectors with the minor axes of the ellipses in Fig. 4a, b would imply that the polarisation ratios, Eq. (2), would be dominated by the transverse wind gradient terms, which would now be $\left|\frac{1}{N}\frac{dU}{\mathrm{d}z}\right|$.

The wind observations confirm such large values of the gradient terms. It is found that the sign of the gradient term in the troposphere case reproduces the anticlockwise rotation shown in Fig. 4a. However, that for the lower stratosphere case also predicts an anticlockwise rotation in contrast to the clockwise sense actually observed, Fig. 4b. Furthermore, the value of ω for the tropospheric case from expression (4) is indeterminate. It is concluded, therefore, that the present data are not consistent with waves propagating transverse to the jet stream.

A significant feature of the present study is the pronounced wave disturbance observed at heights well below the jet stream maximum, down to the lowest height of observation near 2 km, and of magnitude comparable with that at low stratospheric levels. Previous observations of inertia-gravity waves by balloons (Thompson, 1978; Cadet and Teitelbaum, 1979) and radar (Cornish and Larsen, 1989; Thomas *et al.*, 1992; Sato, 1994; Cho, 1995) show relatively small intensities or even an absence of such disturbances at such heights. A study of the generation of gravity waves by geostrophic adjustment for zonally extended imbalances by Fritts and Luo (1992) shows wave propagation at positions away from the jet, with downward phase progression above and upward phase progression below with no obvious difference in amplitude. The predicted propagation transverse to the jet is generally consistent with previous radar observations showing a preference for meridional propagation of waves in the lower stratosphere. However, some observations question the relation of the observed waves to the jet stream (Sato, 1994). The present observations for lower stratospheric heights are simulated more closely by the modelling study of O'Sullivan and Dunkerton (1995). This shows that inertia-gravity waves generated as the tropospheric jet stream was distorted by baroclinic instability, primarily in the jet stream exit region, were concentrated on the upper side of the jet. As observed in the present study, the waves propagated in a similar direction to the jet stream, and at a lower velocity. The waves showed similar phase surface slopes to those observed at lower stratospheric heights in Fig. 2a, b, had an intrinsic period of 9 h but a period relative to the ground of 14 h, and a value of $2\pi/k$ of 600 km. There is no basis for invoking a separate source such as frontal activity to explain the present tropospheric perturbations in view of the downward propagation of wave energy indicated by the hodographs in the troposphere, as in Fig. 4a, and the general consistency of the results with those for the lower stratosphere.

5 Conclusions

VHF radar measurements at Aberystwyth have shown the presence of inertia-gravity waves during 12–13 March, 1994, with downward phase progression in the

troposphere and upward propagation in the lower stratosphere, the apparent periods being near 9 and 10 h, respectively. These results, together with hodographs of horizontal perturbation velocity, show that in both height regions the observed wave propagation is in directions similar to that of the jet stream, with downward energy flow in the troposphere and upward flow in the lower stratosphere. Allowance for the gradient in the background wind transverse to the direction of wave propagation introduces some uncertainties in the derivation of wave parameters, especially in the lower stratosphere, but an intrinsic period of 7–8 h and a horizontal wavelength of 136–164 km are found for the middle troposphere. The wave characteristics show features which contrast with previous observations of inertia-gravity waves which showed preference for propagation approximately transverse to the jet stream and relatively small intensities or complete absence of waves at middle and lower tropospheric heights.

Acknowledgements. The authors are grateful to Colin Hines for providing valuable comments on the manuscript. The radiosonde data was supplied by the NERC British Atmospheric Data Centre.

Topical Editor J.-P. Duvel thanks U.-P. Hoppe and another referee for their help in evaluating this paper.

References

Cadet, D., and H. Teitelbaum, Observational evidence of internal gravity waves in the tropical stratosphere, *J. Atmos. Sci.*, **36,** 892–907, 1979.

Cho, J. Y. N., Inertia-gravity wave parameter estimation from cross-spectral analysis, *J. Geophys. Res.*, **100,** 18727–18737, 1995.

Cornish, C. R., and M. F. Larsen, Observations of low-frequency inertia-gravity waves in the lower stratosphere over Arecibo, *J. Atmos. Sci.*, **46,** 2428–2439, 1989.

Fritts, D. C., and Z. Luo, Gravity wave excitation by geostrophic adjustment of the jet stream. Part I: two-dimensional forcing, *J. Atmos. Sci.*, **49,** 681–697, 1992.

Hines, C. D., Tropopausal mountain waves over Arecibo: a case study, *J. Atmos. Sci.*, **46,** 476–488, 1989.

Hines, C. D., Modulated mountain waves, *J. Atmos. Sci.*, **52,** 602–606, 1995a.

Hines, C. D., Comments on "Observations of low-frequency inertia-gravity waves in the lower stratosphere over Arecibo", *J. Atmos. Sci.*, **52,** 607–610, 1995b.

Hirota, I., and T. Niki, Inertia-gravity waves in the troposphere and stratosphere observed by the MU radar, *J. Meteorol. Soc., Japan*, **64,** 995–999, 1986.

Kunze, E., Near-inertial wave propagation in geostrophic shear, *J. Phys. Oceanogr.*, **15,** 544–565, 1985.

Larsen, M. F., Reply with comments on "Modulated mountain waves.", *J. Atmos. Sci.*, **52,** 611–612, 1995.

Luo, Z., and D. C. Fritts, Gravity wave excitation by geostrophic adjustment of the jet stream. Part II: three-dimensional forcing, *J. Atmos. Sci.*, **50,** 104–115, 1993.

Maekawa, Y., S. Fukao, T. Sato, S. Kato, and R. F. Woodman, Internal inertia-gravity waves in the tropical lower stratosphere observed by the Arecibo radar, *J. Atmos. Sci.*, **41,** 2539–2545, 1984.

O'Sullivan, D., and T. J. Dunkerton, Generation of inertia-gravity waves in a simulated life cycle of baroclinic instability, *J. Atmos. Sci.*, **52,** 3695–3716, 1995.

Prichard, I. T., and L. Thomas, Radar observations of gravity-wave momentum fluxes in the troposphere and lower stratosphere, *Ann. Geophysicae*, **11,** 1075–1083, 1993.

Prichard, I. T., L. Thomas, and R. M. Worthington, The characteristics of mountain waves observed by radar near the west coast of Wales, *Ann. Geophysicae*, **13,** 757–767, 1995.

Sato, K., A statistical study of the structure, saturation and sources of inertia-gravity waves in the lower stratosphere observed with the MU radar, *J. Atmos. Terr. Phys.*, **56,** 755–774, 1994.

Sato, T., and R. F. Woodman, Fine altitude resolution radar observations of upper-tropospheric and lower stratospheric winds and waves, *J. Atmos. Sci.*, **39,** 2539–2545, 1982.

Thomas, L., I. T. Prichard, and I. Astin, Radar observations of an inertia-gravity wave in the troposphere and lower stratosphere, *Ann. Geophysicae*, **10,** 690–697, 1992.

Thompson, R. O. R. Y., Observation of inertial waves in the stratosphere, *Q.J.R. Meteorol. Soc.*, **104,** 691–698, 1978.

Tsuda, T., S. Kato, T. Yokoi, T. Inoue, M. Yamamoto, T. E. VanZandt, S. Fukao, and T. Sato, Gravity waves in the mesosphere observed with the middle and upper atmosphere radar, *Radio Sci.*, **26,** 1005–1018, 1990.

Worthington, R. M., and L. Thomas, Radar measurements of critical-layer absorption in mountain waves, *Q.J.R. Meteorol. Soc.*, **122,** 1263–1282, 1996.

Yamanaka, M. D., S. Fukao, H. Matsumoto, T. Sato, T. Tsuda, and S. Kato, Internal gravity wave selection in the upper troposphere and lower stratosphere observed by the MU radar: preliminary results, Pure *Appl. Geophys.*, **130,** 481–495, 1989.